J|A|C|S
COMMUNICATIONS

Published on Web 12/07/2006

Water Penetration into Protein Secondary Structure Revealed by Hydrogen−Deuterium Exchange Two-Dimensional Infrared Spectroscopy

Lauren P. DeFlores and Andrei Tokmakoff*

Department of Chemistry, Massachusetts Institute of Technology, Cambridge, Massachusetts 02139

Received October 29, 2006; E-mail: tokmakof@mit.edu

Hydrogen−deuterium exchange (HX) is a valuable tool for characterizing protein structural stability, solvation and water exposure, and unfolding kinetics.[1,2] HX is influenced by the site-specific pK_a, solvent accessibility to protonated sites, and strength of hydrogen-bonding interactions.[1] In the hydrophobic core or strongly hydrogen-bound secondary structures, HX rates are dramatically reduced due to shielding of exchangeable sites.[1] NMR methods infer the degree of protection and structural stability from site-specific HX measurements,[3,4] which can be incorporated into fast-mixing experiments to provide information about reaction intermediates.[1] IR spectroscopy in conjunction with HX also provides information on solvent exposure of the protein backbone, relying on the strong red shift of the amide II (AmII) vibration upon deuteration of the peptide group NH.[5] IR is an appealing technique for kinetic studies, since it can be used in combination with fast unfolding experiments.[6,7] However, AmII is not otherwise structurally sensitive and is typically overlapped with side-chain absorptions. Using two-dimensional infrared (2D IR) spectroscopy, we have performed HX experiments that combine the solvent-exposure sensitivity of AmII with the secondary-structure sensitivity of amide I (AmI). The correlation of transition frequencies in the AmI−II region provides a secondary structure-sensitive probe of protein solvent accessibility ideal for studies of protein folding and stability.

2D IR spectroscopy of AmI vibrations has found wide use in the study of protein and small-peptide conformation and dynamics.[8,9] In the case of proteins, the coupling between AmI vibrations of individual peptide groups leads to excitonic states whose vibrational spectrum reflects the symmetry of underlying secondary structures and the extent of delocalization.[9,10] In FTIR spectra, antiparallel β-sheets give rise to a two-peak AmI signature located at ∼1630 cm^{-1} ($\nu_\perp$) and ∼1690 cm^{-1} ($\nu_\parallel$), while α-helical and random coil absorptions overlap in the middle of the AmI band (∼1650 cm^{-1}). 2D IR spectroscopy of proteins has provided a higher level of detail about protein backbone conformation and secondary structure and is finding use in folding studies.[11,12]

2D IR experiments can be extended to dissect the AmI spectral profile on the basis of the solvent exposure of secondary structures. For proteins immersed in D_2O, buried residues that remain protonated will absorb at ∼1550 cm^{-1} (AmII), while solvent-exchanging (deuterated) residues will absorb at ∼1450 cm^{-1} (AmII'). The position and shape of AmI−II cross-peaks correlates the secondary structure observed by AmI vibrations with the protonation state of AmII, isolating solvent-inaccessible secondary structures and hydrophobic regions of the protein. We have investigated the AmI−II 2D IR spectra for several proteins with varying secondary structure motifs. Figure 1 shows the results for four proteins: concanavalin A (Con A), myoglobin, ribonuclease A (RNaseA), and ubiquitin. Additional protein spectra are presented in the Supporting Information.

Resonances in the 2D IR spectrum correlate the frequency of vibrational excitation ω_1 with the detection frequency ω_3 and appear as an oppositely signed doublet.[13] The diagonal features ($\omega_1 = \omega_3$) can be assigned to components in the FTIR spectrum and are diagonally elongated as a result of inhomogeneous broadening. Off-diagonal intensity arises from vibrational coupling. The AmI portion of the spectrum contains distinctive line shapes that arise from interference effects and indicate the underlying secondary structure content. Z-shaped contour profiles elongated along $\omega_3 = \nu_\perp$ and $\nu_\parallel$ are characteristic of β-sheets and are observed for Con A, RNaseA, and ubiquitin.[12] The diagonal AmII peak is observed at ∼1550 cm^{-1}, and additional diagonal features between 1550 and 1610 cm^{-1} arise from side-chain absorptions by Asp, Glu, Asn, Gln, and Arg.[14] Each of the protein spectra exhibit cross-peaks between the AmI and AmII vibrations with strongly varying line shapes. Since AmI and AmII vibrations are anharmonically coupled,[15] these cross-peaks arise from couplings in nonexchanged residues of the protein and directly reveal the AmI spectrum of the buried, nonexchanging residues and secondary structures of the protein. The cross-peaks are observed to extend along ω_1 with the width of AmII and with ω_3 peaks that pick out components from the AmI diagonal feature.

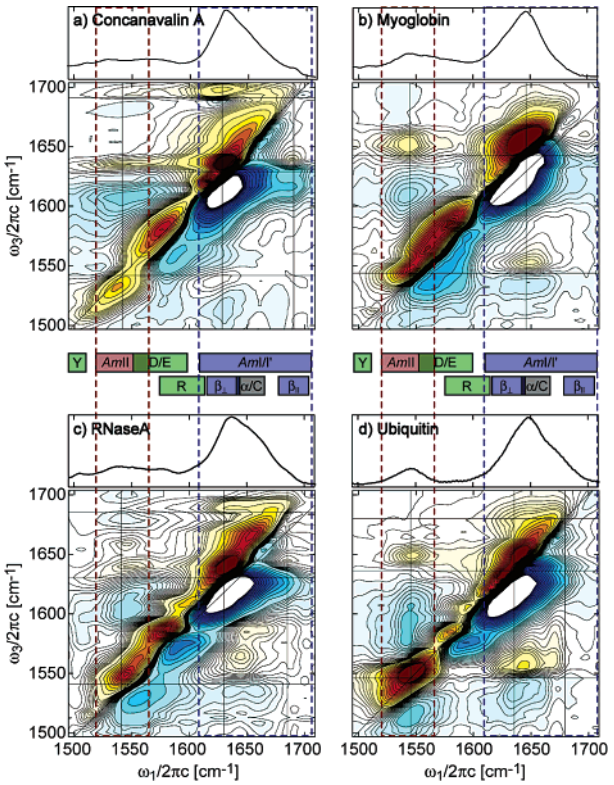

Figure 1. FTIR and absorptive amide I/I′−II 2D IR spectra of (a) Con A, (b) myoglobin, (c) RNaseA, and (d) ubiquitin. The spectral regions corresponding to the AmI/I′, AmII, and various side-chain absorptions are labeled in the middle. Dashes mark the AmI and AmII regions over which the slices in Figure 2 were integrated.

10.1021/ja067723o CCC: $33.50

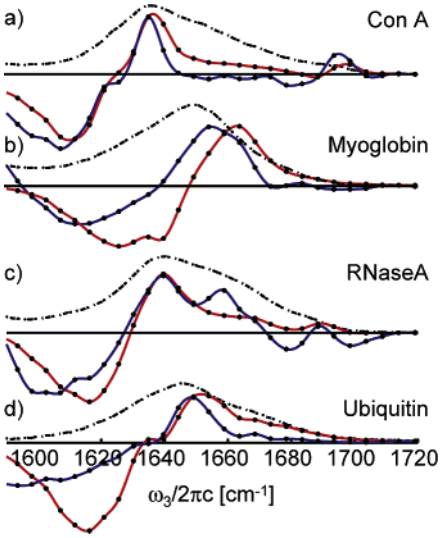

Figure 2. Normalized slices taken along $\omega_1 = \omega_{AII}$ (blue) overlapped with the AmI slice (red) and Am I FTIR (black dashed).

To analyze these cross-peaks, slices for $\omega_1 = \omega_{AII}$ integrated over a 30 cm^{-1} window in ω_1 are plotted in Figure 2. These are compared to the AmI FTIR and the AmI diagonal region projected onto ω_3. For Con A, a β-protein, the cross-peak consists of a pair of vertically displaced doublets at $\omega_3 = 1630$ and 1690 cm^{-1} (Figure 1a), indicative of its antiparallel β-sheets. The lack of intensity between 1640 and 1680 cm^{-1}, seen in the cross-peak slice of Figure 2a, indicates that coil and turn regions at the edge of the protein have exchanged. The cross-peak for myoglobin, an α-protein, shows a highly rounded and intense doublet centered at $\omega_3 = 1646$ cm^{-1}. The peak is red-shifted from the main AmI band, suggesting a loss of spectral content from coil contributions. This allows one to clearly isolate secondary structural elements from the random coil and solvent-exposed regions of the protein. Previous HX studies on RNaseA, an α/β-protein, concluded that secondary structural elements contain mixed protonation states.[6] The presence of cross-peaks in the 2D IR spectra containing all of the AmI features implies a high degree of secondary structural stability in RNaseA at pH 7 and 5 °C. The cross-peak slice (Figure 2c) shows distinct signatures of its β-sheet and α-helices.

For ubiquitin, the 2D spectrum in Figure 1d and cross-peak slice in Figure 2d show a round cross-peak centered at the frequency associated with α-helices. This indicates that, even though ubiquitin has a five-stranded mixed sheet, the β-sheet of ubiquitin is relatively labile and exchanges readily under low pH and temperature, and the protons of the helix are least susceptible to HX. This conclusion is consistent with ubiquitin unfolding studies, which argue that ubiquitin's mixed β-sheet is partially disordered at the unfolding transition state. The first 37 residues form a tightly folded core consisting of a hairpin and helix,[4] whereas the remaining three strands of the sheet are presumed to be less stable and unfold first.[11]

The side-chain spectral features provide further insight into solvent exposure within these proteins. In the 1570−1610 cm^{-1} ubiquitin window is observed a pair of sharp diagonal peaks with ω_3-elongated ridges indicating cross-peaks. We assign this feature to the coupled symmetric/asymmetric guanidinium vibrations of the Arg side chains.[14] The two modes appear at this frequency only on deuterating the side chain, and they persist on full HX, indicating that they are solvent-exposed (Figure S2 in the Supporting Information). In the case of ubiquitin, the four arginines present are within the loops and termini of the destabilized β-strands. Similar features are observed in RNaseA and lysozyme.

In addition to the structural sensitivity of the technique, 2D IR provides information about the protein anharmonic vibrational potential. These spectra, particularly for α-proteins, show cross-peak splittings that give a large apparent off-diagonal anharmonicity or coupling strength. This feature most likely arises more from the inhomogeneous broadening of AmI; however, this opens questions about the degree of amide mode coupling in proteins.[16] Another feature, particularly in the β-sheet containing proteins, is the asymmetry of the upward ($\omega_1 < \omega_3$) and downward ($\omega_1 > \omega_3$) cross-peaks. The asymmetry can be explained by destructive interference effects between vertically elongated positive and negative cross-peaks. The intensity mismatch is less dramatic in the case of myoglobin and ubiquitin.

In conclusion, H/D exchange 2D IR spectroscopy can be used to isolate spectra for buried secondary structure elements through vibrational coupling of the AmI and AmII modes. Coupling of the amide modes in these isolated regions shows distinct spectral features indicative of α-helical and/or β-sheet structure, implying a high degree of stability of hydrogen-bonding contacts. With further advances to expand femtosecond IR pulse bandwidths, the AmI, AmII, and AmII′ modes can be simultaneously probed, providing a clear separation of solvent-accessible and -inaccessible residues. Further, one can imagine experiments that use these probes for fast time-resolved protein unfolding kinetics.

Acknowledgment. This work was supported by the National Science Foundation (CHE-0316736 and CHE-0616575).

Supporting Information Available: Sample preparation; data analysis; and additional 2D spectra of lysozyme, serum albumin, β-lactoglobulin, and partially and fully exchanged ubiquitin. This material is available free of charge via the Internet at http://pubs.acs.org.

References

(1) Englander, S. W.; Sosnick, T. R.; Englander, J. J.; Mayne, L. C. *Curr. Opin. Struct. Biol.* **1996**, *6*, 18−23.
(2) Grdadolnik, J.; Marechal, Y. *Appl. Spectrosc.* **2005**, *59*, 1357.
(3) Bai, Y.; Sosnick, T. R.; Mayne, L. C.; Englander, S. W. *Science* **1995**, *269*, 192−197.
(4) Briggs, M. S.; Roder, H. *Proc. Natl. Acad. Sci. U.S.A.* **1992**, *89*, 2017−2021.
(5) Dyer, R. B.; Gai, F.; Woodruff, W. H.; Gilmanshin, R.; Callender, R. H. *Acc. Chem. Res.* **1998**, *31*, 709−716.
(6) Dong, A.; Hyslop, R. M.; Pringle, D. L. *Arch. Biochem. Biophys.* **1996**, *333*, 275−281.
(7) Wu, Y.; Murayama, K.; Ozaki, Y. *J. Phys. Chem. B* **2001**, *105*, 6251−6259.
(8) (a) Hamm, P.; Lim, M.; Hochstrasser, R. M. *J. Phys. Chem. B* **1998**, *102*, 6123−6138. (b) Woutersen, S.; Hamm, P. *J. Phys.: Condens. Matter* **2002**, *14*, 1035−1062. (c) Mukherjee, P.; Krummel, A. T.; Fulmer, E. C.; Kass, I.; Arkin, I. T.; Zanni, M. T. *J. Chem. Phys.* **2004**, *120*, 10215−10224. (d) Mu, Y.; Stock, G. *J. Phys. Chem. B* **2002**, *106*, 5294−5301. (e) Jansen, T.; Knoester, J. *J. Phys. Chem. B* **2006**, *110*, 22910−22916.
(9) Abramavicius, D.; Zhuang, W.; Mukamel, S. *J. Phys. Chem. B* **2004**, *108*, 18034−18045.
(10) Chung, H. S.; Tokmakoff, A. *J. Phys. Chem. B* **2006**, *110*, 2888−2898.
(11) Chung, H. S.; Khalil, M.; Smith, A. W.; Ganim, Z.; Tokmakoff, A. *Proc. Natl. Acad. Sci. U.S.A.* **2005**, *102*, 612−617.
(12) Demirdöven, N.; Cheatum, C. M.; Chung, H. S.; Khalil, M.; Knoester, J.; Tokmakoff, A. *J. Am. Chem. Soc.* **2004**, *126*, 7981−7990.
(13) Khalil, M.; Demirdoven, N.; Tokmakoff, A. *J. Phys. Chem. A* **2003**, *107*, 5258−5279.
(14) (a) Barth, A.; Zscherp, C. *Q. Rev. Biophys.* **2002**, *35*, 369−430. (b) Chirgadze, Y. N.; Fedorov, O. V.; Trushina, N. P. *Biopolymers* **1975**, *14*, 679.
(15) DeFlores, L. P.; Ganim, Z.; Ackley, S. F.; Chung, H. S.; Tokmakoff, A. *J. Phys. Chem. B* **2006**, *110*, 18973−18980.
(16) Hayashi, T.; Zhuang, W.; Mukamel, S. *J. Phys. Chem. A* **2005**, *109*, 9757−9759.

JA067723O